SCIENTIFIC REPORT

Abnormal crossing of the optic fibres shown by evoked magnetic fields in patients with ocular albinism with a novel mutation in the *OA1* gene

L Lauronen, R Jalkanen, J Huttunen, E Carlsson, S Tuupanen, S Lindh, H Forsius, E-M Sankila, T Alitalo

Br J Ophthalmol 2005;**89**:820–824. doi: 10.1136/bjo.2004.060582

Aim: To perform genealogical and clinical studies in Finnish families with X linked ocular albinism (OA1), including characterisation of the potential misrouting of optic fibres by evaluating visual evoked magnetic fields (VEFs), and to determine the mutation behind the disease.
Methods: Three families with OA1 were clinically examined. VEFs were measured in two affected males and in one female carrier to characterise the cortical activation pattern after monocular visual stimulation. The neuronal sources of the VEFs were modelled with equivalent current dipoles (ECDs) in a spherical head model. All coding exons of the *OA1* gene were screened for mutations by single strand conformation analysis and direct polymerase chain reaction sequencing.
Results: Genealogical studies revealed that the three families were all related. The affected males had foveal hypoplasia with reduced visual acuity varying from 20/200 to 20/50, variable nystagmus, iris transillumination, and hypopigmentation of the retinal pigment epithelium. The ECD locations corresponding to the VEFs revealed abnormal crossing of the optic fibres in both affected males, but not in the carrier female. A novel point mutation, leading to a STOP codon, was identified in the fifth exon of the *OA1* gene.
Conclusions: The data indicate that the novel mutation 640C>T in the *OA1* gene is the primary cause of the eye disease in the family studied. VEFs with ECD analysis was successfully used to demonstrate abnormal crossing of the optic fibres.

The X chromosomal Nettleship-Falls type ocular albinism (OA1; OMIM 300500) is the most common form of ocular albinism with a prevalence of 1 in 60 000 live births.[1] Affected males have reduced visual acuity, nystagmus, iris translucency, fundus hypopigmentation, foveal hypoplasia, and loss of stereoscopic vision.[2–5] Skin colour of the patients appears to be normal.[4 6] The disease results from abnormal distribution of melanin. Microscopic examination of histological samples typically reveals macromelanosomes in pigment cells of skin and eye.[7 8] Carrier females are usually asymptomatic, but because of random X inactivation,[9] the majority of them show some signs of carriership including pigment changes in the fundus, iris translucency, and macromelanosomes in skin biopsy.[10–12]

The disease phenotype results from mutations in the *OA1* gene (albinism database: albinismdb.med.umn.edu/). The gene has been localised to Xp22.32,[13–16] and it consists of nine exons, encoding a protein of 404 amino acids.[17 18] The *OA1* gene product is an intracellular G protein coupled receptor that localises to melanosomes, and is shown to be involved in melanosome biogenesis and maturation.[19–21]

A typical feature of ocular albinism is abnormal crossing of the visual pathways at the chiasma: the majority of the fibres from each eye cross to the contralateral hemisphere, while in healthy subjects, only fibres from the nasal half of the retina cross. Accordingly, abnormal lateralisation of visual evoked potentials (VEPs) to monocular stimulation has been reported in ocular albinism,[22–25] although in some studies no abnormal lateralisation has been found.[26] A potential difficulty in evaluating VEP studies is that these have usually been recorded from a limited number of channels, which precludes accurate estimation of the underlying neuronal generators. In magnetoencephalography (MEG), the active brain areas are detected by recording the weak magnetic fields caused by activation of neuronal populations at the cortex.[27] In contrast with electric potentials, the magnetic fields are not altered by the different conductivities of the intervening tissues. Therefore, with multichannel MEG devices, the accurate location and strength of the neuronal generators of evoked responses can frequently be determined. Thus, it is possible—for example, by recording visual evoked magnetic fields (VEFs), to determine whether a half field visual stimulus activates the visual cortex ipsilaterally or contralaterally to the stimulated eye. We have previously reported preliminary results to half field checkerboard stimulation in patients with ocular albinism.[28] Recently, Ohde *et al*[29] used VEFs to show misrouting of the optic fibres in one patient with ocular albinism and two patients with oculocutaneous albinism. However, they used stroboscopic light with monocular or binocular stimulation instead of half field stimulation.

This study was conducted to evaluate clinical findings, including characterisation of the misrouting of the optic fibres with VEFs, in patients with X chromosomal ocular albinism. Molecular genetic analysis of the *OA1* gene was performed to determine the mutation behind the disease.

MATERIALS AND METHODS

Clinical studies

Subjects and ophthalmic examination

Patients and carriers belonging to the three families (descendants of VII-2, VII-5, and VII-10, fig 1) were clinically studied. Ocular examinations were performed using a Haag-Streit slit lamp microscope and a 90 D or a three mirror lens. Since the patients of the three families appeared to have both

Abbreviations: ECD, equivalent current dipole; MEG, magnetoencephalography; OA, ocular albinism; PCR, polymerase chain reaction; RPE, retinal pigment epithelium; SSCA, single strand conformation analysis; VEF, visual evoked magnetic field; VEP, visual evoked potential

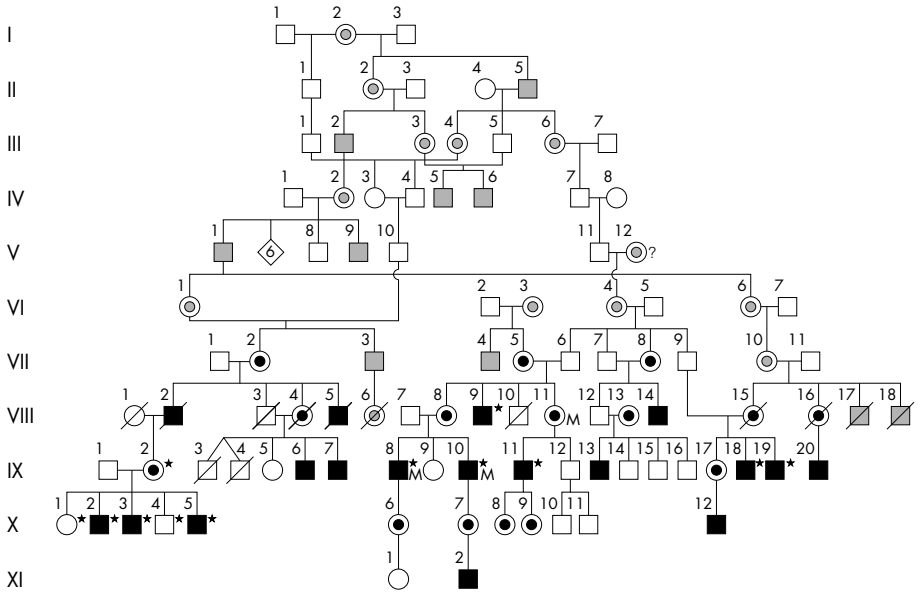

Figure 1 Pedigree of the Finnish OA1 family. Members of the I–VII generation are all dead, generations VIII–XI as shown. *Indicates individuals who took part in molecular studies. M, patients examined by magnetoencephalography. Black squares, affected males; shaded squares, males having poor eyesight according to church registers; open circles with a black dot, carrier females; and open symbols, unaffected individuals. Question mark indicates that the phenotype is unknown.

a similar phenotype and ancestors from the island of Seiskari, we initiated genealogical studies using church registers to find out whether the families are related.

Magnetoencephalography

Two brothers (IX-8 and IX-10) with OA1, one carrier female (VIII-11), and five healthy control subjects (age range 23–51 years) underwent VEF studies. The two patients and all controls were measured with a 122 channel gradiometer (Neuromag Ltd, Helsinki, Finland) and the carrier with a 306 channel system (Elekta Neuromag, Oy, Helsinki, Finland), located inside a magnetically shielded room. The subject sat with his/her head positioned inside the helmet-shaped sensor array, and watched a fixation point in the middle of the stimulus screen placed 1.5 metres in front of him/her. The nasal and temporal visual half fields of the left and right eye were stimulated separately with a black and white checkerboard pattern reversing at 1 Hz. The check size was approximately 3°. Two sets of 200 responses were averaged for both half fields of both eyes. The signals were band pass filtered between 0.1 Hz and 200 Hz and sampled at 616 Hz. Epochs containing amplitudes exceeding 3000 fT/cm in the MEG channels or 150 μV in the electro-oculogram were automatically discarded. An epoch lasted 600 ms, including a 100 ms prestimulus baseline. The evoked local cortical activity was modelled with equivalent current dipoles (ECDs), representing the location, orientation, and strength of localised cortical activation.[27] The ECD locations were given in a cartesian head coordinate system, were the x axis passes through the preauricular points from left to right, the positive y axis passes through nasion, and the z axis points upwards. The ECDs at the time of the most prominent activity (at about 100 ms after stimulus) were used in the analyses.

Molecular studies

DNA was extracted from blood samples using standard methods. All nine coding exons of *OA1* were polymerase chain reaction (PCR) amplified from genomic DNA. Mutation analysis was carried out using single strand conformation analysis (SSCA),[30 31] and direct PCR sequencing (ABI310, Applied Biosystems, Foster City, CA, USA).

RESULTS

Genealogical studies and clinical data

The three families were traced back to the 18th century using church registers. A common forefather, born on the island of Seiskari in 1700, was identified (fig 1). Of the eight males studied, seven had foveal hypoplasia and hypopigmented fundi with visible choroidal vessels (table 1). Male IX-11 had foveal hypoplasia but normally pigmented fundi. Optic discs were slightly or markedly pale in four males. Male XI-2 had congenital nystagmus and strabismus and was first examined as a baby. His VEP recordings suggested misrouting of the optic fibres. All the six clinically studied carriers showed some carrier manifestations (table 2).

Table 1 Clinical findings of eight affected males

Pedigree code	Age (years)	Nystagmus	Iris translucency	VA R//L	Refractive error (D) R/L
VIII-9	74	(+)*	−	20/125//20/125	+−0 −2.5×50†/+1.5 −1.0×105
IX-8	44	(+)*	+	20/60//20/50	−2.5 −4.0×5/−1.0 −2.0×180
IX-10	49	+	+	20/100//20/100	+2.25 −6.0×160/+2.25 −4.5×30
IX-11	50	+	+	20/100//20/100	+−0 −3.5×15/+1.5 −3.0×160
X-2	50	+	+	20/60//20/60	+3.25 −2.25×25/+3.25 −2.0×170
X-3	51	+	+	20/200//20/200	+5.0 −1.0×170/+4.5 −1.0×30
X-5	54	+	+	20/100//20/100	−2.75 −2.0×20/−3.0 −2.25×170
XI-2	5	+	+	20/160//20/100	+6.5 −1.0×170/+6.25 −1.0×0

*Low frequency nystagmus at lateral gaze.
†Refraction after cataract surgery.
VA, visual acuity; R/L, right and left eye; D, dioptre.

Table 2 Clinical findings in six female carriers

Pedigree code	Age (years)	Iris translucency	Fundus appearance	VA R//L	Refractive error (D) R/L
VIII-8	70	−	Patchy peripheral RPE	20/60*//20/20	+2.25 −1.5×100/+3.0 −1.75×75
VIII-11	72	−	Patchy RPE	20/20//20/20	+1.75 −0.5×130/+1.5 −0.5×90
IX-2	71	+	Patchy RPE	20/25//20/20	−9.0 −0.5×180/−9.0
X-7	23	+	Normal	20/20//20/20	+−0/+−0
X-8	15	+	Patchy RPE	20/20//20/20	+−0/+−0
X-9	12	+	Patchy RPE	20/20//20/30†	−9.5/−5.75

*Macular pucker.
†Anisometropic amblyopia.
VA, visual acuity; R/L, right and left eye; D, dioptre; RPE, retinal pigment epithelium.

Magnetoencephalography

The monocular half field checkerboard stimulation resulted in responses over the occipital area in both controls and patients (fig 2). For stimulation of either eye, in all controls and in the carrier female, the maximum activation was over the left hemisphere for the right half field stimulation, and over the right hemisphere for the left half field stimulation. In the patients, both left and right half field stimulation resulted in activation over the contralateral hemisphere. The most prominent deflection peaked at about 100 ms (table 3) and was designated as P100m, in analogy to the P100 VEP component. The topographic P100m magnetic field distributions showed dipolar patterns (fig 3), indicating that the P100m was generated by localised cortical activity amenable to modelling with an ECD. In the patients, the P100m ECD to both left and right half field stimulation of the left eye was in the right visual cortex ($x>0$, table 3). The ECD source locations after stimulation of both half fields were close to each other in the patients, while a clear difference in the lateral direction (on the average 42 mm, table 3) was found in the controls. In the patients, the ECD strength was similar to that in the controls for the temporal half field with normally crossing fibres, but clearly weaker for the nasal half field, which showed abnormal crossing (table 3, fig 3).

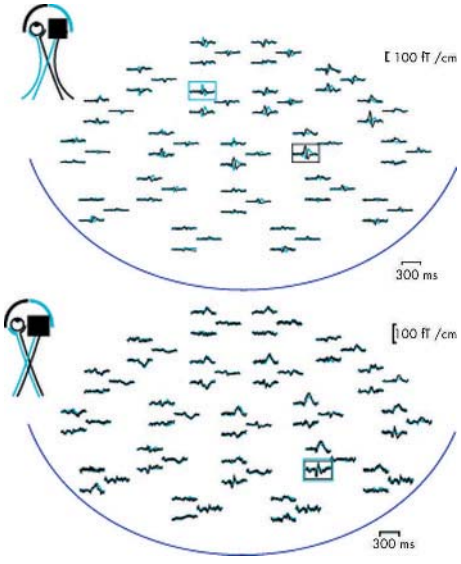

Figure 2 Visual evoked magnetic fields (VEFs) to stimulation of the left eye in a control (top) and in patient IX-8 (bottom). In the control, the nasal half field stimulation (blue line) resulted in maximum activation over the ipsilateral occipital area (blue box) and temporal half field stimulation (black line) over the contralateral occipital areas (black box). In the patient, the maximum responses to stimulation of both half fields were over the contralateral visual cortex; in fact, the responses to both half field stimulations were almost identical. The schematic illustration on the left depicts the corresponding organisation of the optic pathways from the two halves of the retinal to the visual cortex.

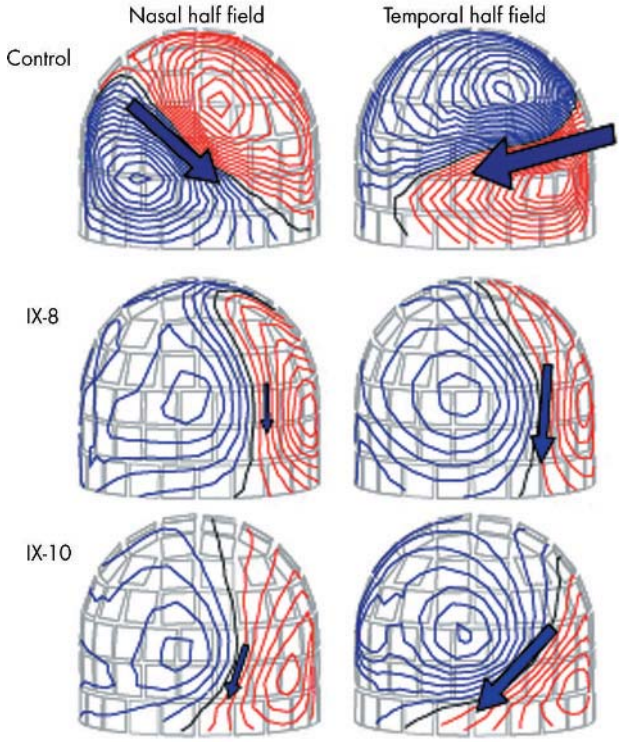

Figure 3 Isofield contour maps showing the topographic magnetic field distribution at the peak of the P100m VEF deflection. The blue lines indicate magnetic flux entering the head and red lines magnetic flux exiting the head. Data from a control subject are shown at the top and from the two patients in the middle and at the bottom after stimulation of the left eye. In the control, the response to nasal half field stimulation was located ipsilaterally in the left hemisphere, whereas the temporal half field stimulation resulted in activation over the contralateral right hemisphere. In both patients, both the nasal and temporal half field stimulation caused activation over the contralateral right hemisphere. The arrows denote the corresponding ECDs, size of the arrow being proportional to the ECD strength. The contour step is 20 fT/cm.

Mutation analysis

Sequence analysis revealed a novel base substitution, 640C>T, in the fifth exon of the *OA1* gene. This substitution changes the glutamine at position 214 to a stop codon. The mutation co-segregated with the disease phenotype in the Finnish family and was not found in 140 normal male control samples.

Table 3 The mean latencies, locations, and strengths of P100m ECDs for stimulation of the left eye in patients and controls. The standard deviations are in parentheses

Subjects	Stimulus	Latency (ms)	Coordinates x (mm)	y (mm)	z (mm)	Strength (nAm)	g %
Patients (n = 2)	Left HF	99 (1)	20 (3)	−54 (2)	42 (2)	23 (5)	92 (5)
	Right HF	100 (3)	26 (1)	−59 (1)	50 (1)	9 (4)	88 (8)
Controls (n = 5)	Left HF	103 (9)	34 (5)	−57 (18)	57 (7)	19 (17)	88 (2)
	Right HF	106 (11)	−8 (5)	−57 (14)	56 (11)	16 (12)	92 (4)

g = goodness of fit (indicates how much of the variance in the recorded signal set is explained by the ECD model), HF = half field, ECD = equivalent current dipole. A positive value of the x coordinate indicates right hemisphere, while negative x falls in the left hemisphere.

DISCUSSION

In this study of a large Finnish family, we identified a novel *OA1* mutation, 640C>T, which leads to a truncated protein product. The predicted mutant protein lacks the putative transmembrane regions VI and VII, part of the transmembrane region V, and also the third sytosolic loop, which may be crucial for downstream signalling of the protein.[32] The mutation resulted in reduced visual acuity in all affected males studied, although iris translucency was absent in one patient, and hypopigmentation of the retina in another. Preising *et al*[33] have hypothesised that in OA1, pigmentation of the iridal and the retinal pigment epithelium may increase postnatally because of constant melanin production of melanocytes, while the neuroretinal phenotype resulting in reduced visual acuity is permanent as a result of irreversible damage during embryogenesis. All the female carriers of the 640C>T mutation studied here had at least some clinical carrier manifestations, but normal visual acuity and normal VEF responses indicating that the routing of optic pathways was not altered

The optic fibre misrouting in OA1 patients was demonstrated by using VEFs with ECD analysis. The patients' main VEF response to stimulation of the nasal half fields was clearly abnormally lateralised to the contralateral hemisphere. Recently, Ohde *et al*[29] found a predominantly contralateral VEF activation pattern in the occipital cortex of three patients with albinims after full field stroboscopic stimulation. This was in contrast with healthy controls in whom full field stimulation led to more ambiguous activation pattern indicating activation of the visual cortex bilaterally. Hence, the authors could infer an abnormal crossing of the optic fibres in the patients. In the present study, we have shown perhaps more directly with checkerboard half field stimulation that both hemifields indeed projected to the contralateral visual cortex.

Our results suggest that VEFs to half field stimulation could be used as a diagnostic tool to reveal abnormal crossing of optic fibres in patients suspected of having ocular albinism.

ACKNOWLEDGEMENTS

The authors thank the families with members affected by ocular albinism for participation and Dr Ilkka Kaitila for the help in collecting samples.

Authors' affiliations

L Lauronen*, J Huttunen, BioMag Laboratory, Helsinki University Central Hospital, Helsinki, Finland
L Lauronen, Helsinki Brain Research Centre, Helsinki, Finland
L Lauronen, J Huttunen, Department of Clinical Neurophysiology, Helsinki University Central Hospital, Helsinki, Finland
R Jalkanen*, E Carlsson, S Tuupanen, T Alitalo, Department of Obstetrics and Gynecology, Helsinki University Central Hospital, Helsinki, Finland
S Lindh, H Forsius, E-M Sankila, The Folkhälsan Institute of Genetics, Department of Molecular Genetics, Helsinki, Finland
E-M Sankila, Department of Ophthalmology, Helsinki University Central Hospital, Helsinki, Finland

*These authors contributed equally to this work.

Funding: This study was supported by the Helsinki University Hospital Grant, TYH1338 (TA), and the Finnish Eye Foundation (E-MS).

Competing interests: No commercial relationships for any authors.

Ethical approval: The study conformed to the tenets of the Declaration of Helsinki. Informed consent was obtained from all participants in accordance with the requirements of the Helsinki University Central Hospital, Department of Ophthalmology Ethics Committee.

Correspondence to: Tiina Alitalo, Helsinki University Central Hospital, Department of OB/GYN, Genetics, Haartmaninkatu 2, PO Box 140, Helsinki, 00029 HUS, Finland; tiina.alitalo@hus.fi

Accepted for publication 9 November 2004

REFERENCES

1 **Rosenberg T**, Schwartz M. X-linked ocular albinism: prevalence and mutations—a national study. *Eur J Hum Genet* 1998;**6**:570–7.
2 **Charles SJ**, Green JS, Grant JW, *et al*. Clinical features of affected males with X linked ocular albinism. *Br J Ophthalmol* 1993;**77**:222–7.
3 **Creel DJ**, Summers CG, King RA. Visual anomalies associated with albinism. *Ophthalmic Paediatr Genet* 1990;**11**:193–200.
4 **Kriss A**, Russell-Eggitt I, Harris CM, *et al*. Aspects of albinism. *Ophthalmic Paediatr Genet* 1992;**13**:89–100.
5 **King RA**, Hearing VJ, Creel DJ, *et al*. Albinism. In: Scriver CR, Beaudet AL, Sly WS, *et al*, eds. *The metabolic and molecular bases of inherited disease*. New York: McGraw-Hill, 2001:5587–627.
6 **Creel D**, O'Donnell FE Jr, Witkop CJ Jr. isual system anomalies in human ocular albinos. *Science* 1978;**201**:931–3.
7 **O'Donnell FE Jr**, Hambrick GW Jr, Green WR, *et al*. X-linked ocular albinism. An oculocutaneous macromelanosomal disorder. *Arch Ophthalmol* 1976;**94**:1883–92.
8 **Garner A**, Jay BS. Macromelanosomes in X-linked ocular albinism. *Histopathology* 1980;**4**:243–54.
9 **Lyon MF**. Sex chromatin and gene action in the mammalian X-chromosome. *Am J Hum Genet* 1962;**14**:135–48.
10 **Charles SJ**, Moore AT, Grant JW, *et al*. Genetic counselling in X-linked ocular albinism: clinical features of the carrier state. *Eye* 1992;**6**:75–9.
11 **Cortin P**, Tremblay M, Lemagne JM. X-linked ocular albinism: relative value of skin biopsy, iris transillumination and funduscopy in identifying affected males and carriers. *Can J Ophthalmol* 1981;**16**:121–3.
12 **Lang GE**, Rott HD, Pfeiffer RA. X-linked ocular albinism. Characteristic pattern of affection in female carriers. *Ophthalmic Paediatr Genet* 1990;**11**:265–71.
13 **Bergen AA**, Zijp P, Schuurman EJ, *et al*. Refinement of the localization of the X-linked ocular albinism gene. *Genomics* 1993;**16**:272–3.
14 **Fialkow PJ**, Giblett ER, Motulsky AG. Measurable linkage between ocular albinism and Xg. *Am J Hum Genet* 1967;**19**:63–9.
15 **Pearce WG**, Sanger R, Race RR. Ocular albinism and Xg. *Lancet* 1968;**1**:1282–3.
16 **Schnur RE**, Nussbaum RL, Anson-Cartwright L, *et al*. Linkage analysis in X-linked ocular albinism. *Genomics* 1991;**9**:605–13.
17 **Schiaffino MV**, Bassi MT, Galli L, *et al*. Analysis of the OA1 gene reveals mutations in only one-third of patients with X-linked ocular albinism. *Hum Mol Genet* 1995;**4**:2319–25.
18 **Bassi MT**, Schiaffino MV, Renieri A, *et al*. Cloning of the gene for ocular albinism type 1 from the distal short arm of the X chromosome. *Nat Genet* 1995;**10**:13–19.
19 **Schiaffino MV**, Baschirotto C, Pellegrini G, *et al*. The ocular albinism type 1 gene product is a membrane glycoprotein localized to melanosomes. *Proc Natl Acad Sci USA* 1996;**93**:9055–60.
20 **Shen B**, Rosenberg B, Orlow SJ. Intracellular distribution and late endosomal effects of the ocular albinism type 1 gene product: consequences of

disease-causing mutations and implications for melanosome biogenesis. *Traffic* 2001;**2**:202–11.
21 **Schiaffino MV**, d'Addio M, Alloni A, *et al*. Ocular albinism: evidence for a defect in an intracellular signal transduction system. *Nat Genet* 1999;**23**:108–12.
22 **Creel D**, Witkop CJ Jr, King RA. Asymmetric visually evoked potentials in human albinos: evidence for visual system anomalies. *Invest Ophthalmol* 1974;**13**:430–40.
23 **Apkarian P**, Reits D, Spekreijse H, *et al*. A decisive electrophysiological test for human albinism. *Electroencephalogr Clin Neurophysiol* 1983;**55**:513–31.
24 **Dorey SE**, Neveu MM, Burton LC, *et al*. The clinical features of albinism and their correlation with visual evoked potentials. *Br J Ophthalmol* 2003;**87**:767–72.
25 **Pott JW**, Jansonius NM, Kooijman AC. Chiasmal coefficient of flash and pattern visual evoked potentials for detection of chiasmal misrouting in albinism. *Doc Ophthalmol* 2003;**106**:137–43.
26 **Bouzas EA**, Caruso RC, Drews-Bankiewicz MA, *et al*. Evoked potential analysis of visual pathways in human albinism. *Ophthalmology* 1994;**101**:309–14.
27 **Hämäläinen M**, Hari R, Ilmoniemi RJ, *et al*. Magnetoencephalography—theory, instrumentation and applications to noninvasive studies of the working human brain. *Rev Mod Phys* 1993;**65**:414–97.
28 **Lauronen L**, Sankila E-M, Salmi T, *et al*. Visual evoked magnetic fields in the detection of optic pathway misrouting in ocular albinism [abstract]. In: *BioMag2002*. Jena, Germany, 2002.
29 **Ohde H**, Shinoda K, Nishiyama T, *et al*. New method for detecting misrouted retinofugal fibers in humans with albinism by magnetoencephalography. *Vis Res* 2004;**44**:1033–8.
30 **Orita M**, Iwahana H, Kanazawa H, *et al*. Detection of polymorphisms of human DNA by gel electrophoresis as single-strand conformation polymorphisms. *Proc Natl Acad Sci USA* 1989;**86**:2766–70.
31 **Bassam BJ**, Caetano-Anolles G, Gresshoff PM. Fast and sensitive silver staining of DNA in polyacrylamide gels. *Anal Biochem* 1991;**196**:80–3.
32 **d'Addio M**, Pizzigoni A, Bassi MT, *et al*. Defective intracellular transport and processing of OA1 is a major cause of ocular albinism type 1. *Hum Mol Genet* 2000;**9**:3011–8.
33 **Preising M**, Op de Laak JP, Lorenz B. Deletion in the OA1 gene in a family with congenital X linked nystagmus. *Br J Ophthalmol* 2001;**85**:1098–103.

ECHO

RP1 mutations cause autosomal recessive retinitis pigmentosa

Please visit the *British Journal of Ophthalmology* website [www.bjophthalmol.com] for a link to the full text of this article.

RP1 gene mutations have been discovered for the first time in autosomal recessive retinitis pigmentosa (RP), according to a study of consanguineous Pakistani families with the condition. They are not a major cause of the disorder in Pakistanis, say the researchers.

All affected members of two families were homozygous at the RP1 locus, whereas their parents and unaffected siblings were heterozygous. A homozygous C→T missense mutation at nucleotide 1118 (thre→isoleu at codon 373) segregated with affected family members. Unaffected members were all heterozygous for the mutation, and 100 ethnically matched, unrelated, healthy controls showed no homozygous mutation. A third family had a homozygous four base pair insertion at 1461–65 TGAA, producing a stop codon and a drastically shortened protein product. Again, the mutation segregated with affected family members; it was present in some other members and parents of affected members as a heterozygous mutation but not in the controls. Affected members of all three families had severe RP and were completely blind by age 18 years. Finally, a new heterozygous G→A missense mutation at nucleotide 2005 (ala→thre at codon 669) was found in one patient in a random panel of 150 patients with RP screened for RP1 mutations, but not in the controls.

All patients, their parents, and some of their unaffected siblings were thoroughly investigated and had electroretinographic examinations. Mutational analysis comprised amplification of DNA from blood samples, heteroduplex analysis, and direct DNA sequencing.

All previously known mutations in the RP1 gene cause autosomal dominant RP.

▲ Khaliq S, *et al*. *Journal of Medical Genetics* 2005;**42**:436–438.